Optica Applicata VIII/1, 1978

*Piotr Becla, Jacek F. Kasprzak, Janusz M. Pawlikowski**

PEM-effect in graded-gap $Cd_xHg_{1-x}Te$ layers

The spectral responses of the photoelectromagnetic effect (PEM) in epitaxial $Cd_xHg_{1-x}Te$ layers with the energy gap gradien at the temperatures ranging between 77 and 300 K have been measured in magnetic fields $0 < B \leqslant 2.5$ Tesla. The short-circuit current of the PEM-effect has been also measured as a function of magnetic field. Thus information concerning the properties of the electric transport in those layers have been obtained and the applicability of the examined elements to the wide-band infrared detectors determined.

1. Introduction

The photoelectromagnetic effect (PEM) was discovered in 1934 by Kikoin and Noskov [1]. The theoretical description of the PEM-effect in semiconductors was presented in many papers (see for instance [2, 3, 4]). Some papers concerning the PEM--effect in the mixed $Cd_xHg_{1-x}Te$ crystals have been also published (for instance [5, 6]), in which the PEM-effect in solid crystalline material have been discussed.

The PEM-effect has been analysed also in non-uniform semiconductors with a gradient of energy gap [7–10]. In particular the theory of the PEM--effect for Cd_xHg_{1-x} Te with an energy gap gradient was presented in [7, 10]. The PEM-effect has been measured in weak magnetic fields, and the analysis of the measurements have been made under assumption that the sample under test exhibits a small gradient of the energy gap. The results obtained were very interesting. They indicate that the examined elements may be used as the detectors for infrared of relatively broad spectral response (see also [19]). The life time of the carriers (electrons) and diffusion length have been determined. However, the theoretical description of the PEM-phenomenon in the semiconductor structure with the energy-gap gradient (and other band parameters) has been based on some simplified assumptions.

Our examination of the physical properties of the mixed $Cd_xHg_{1-x}Te$ crystal and the possibilities of its practical application for detection of infrared radiation have been concentrated so far on the photovoltaic detectors with the *p-n* junction [11]. The present paper contains the results of the PEM-effect, measurements in the epitaxial $Cd_xHg_{1-x}Te$ layers with the energy gap gradient. The results of these examinations have been used to describe the transport effect in the structure with an energy gap gradient, and for the infrared detectors design. These detectors – based on the PEM-effect – appeared to be sensitive within a broad wavelength range and did not require the application of low temperature régime.

2. The PEM-effect in semiconductors with the energy–gap gradient

The PEM-effect consists in creation of a photocurrent or photovoltage in the irradiated semiconductor sample immersed in a magnetic field. In the result of irradiation the excess current carriers appear which diffuse toward the sample inside. These carriers are deflected by magnetic field action, which results in potential difference occurring at the sample ends. After short-circuiting the sample ends a short--circuit current I_{sc} of PEM-effect appears in the external circuit.

The PEM-effect in the semiconductor sample with a energy-gap gradient runs similarly. In such a case, however, the theory describing the PEM--effect is complex. In order to obtain a simple expression for the short-circuit current of PEM-effect it is necessary to accept some drastic assumptions (see [10] for example):

1. The energy-gap gradient is small, i.e. the energy gap changes not more than, for instance, 5% along 1000 lattice constants.

2. The sample is irradiated from the side of broader energy gap.

3. The light intensity is weak and the excitation is bipolar.

*) Institute of Physics, Technical University of Wrocław 50-370 Wrocław, Wybrzeże Wyspiańskiego 27, Poland.

4. There are no space charge and trapping centres in the sample.

5. The surface recombination is negligible with respect to the volume recombination.

6. The magnetic field is very weak (i.e. $\mu B \ll 1$).

On the basis of these assumptions and using both the Onsager relation and continuity equation a simple expression for the short-circuit current I_{sc} of the PEM-effect may be obtained for two cases [10]:

1) Bipolar diffusion length determining by the equation

$$L^2 = \frac{kT}{q}\tau\frac{n_0^{-1}+p_0^{-1}}{[n_0\mu_e(B)]^{-1}+[p_0\mu_h(B)]^{-1}} \tag{1}$$

changes linearly with the distance. Then

$$\frac{B^2}{I_{sc}^2} \sim 1+\delta b+(\mu_e^2+\mu_h^2\delta b)B^2, \tag{2}$$

where B is the magnetic induction value, δ denotes the ratio of equivalent carrier concentrations ($\delta = n_0/p_0$), and b denotes the ratio of electron to hole mobilities ($b = \mu_0/\mu_h$).

2) Effective mass, mobility and concentration are constant, while the energy gap changes as a function of thickness. Then

$$\frac{B}{I_{sc}} \sim 1+\delta b+(\mu_e^2+\mu_h^2\delta b)B^2. \tag{3}$$

The expressions (2) and (3) allow to determine the effective mobility μ_{ef} of the PEM-effect

$$\mu_{ef}^2 = \mu_e^2\frac{1+\delta/b}{1+\delta b}. \tag{4}$$

The above expressions, in spite of the simplifying assumptions, may be convenient for analysis of the experimental results and as such has been used in this work.

3. Results and discussion

3.1. Electrical properties of the samples

Epitaxial $Cd_xHg_{1-x}Te$ layers with the energy gap gradient are produced by the method of epitaxial growth from the gaseous phase [12, 13]. Typical parameters of the technological process were the following: temperature 833 K, layer growth time 100 and 225 hours, the thickness of the layers 500–700 μm. The layers had conductivity of p-type and were usually strongly compensated [13].

The preparation of the samples of requested difference in molar compositions, and required energy gap gradient made by the method of cutting specimens out off the epitaxial layer has been shown in fig. 1. After suitable grinding, polishing and etching the samples obtained were about of $3\times1\times0.1$ mm while the energy gap gradient was of order of 10^4 eV/m, usually within the region of molar compositions

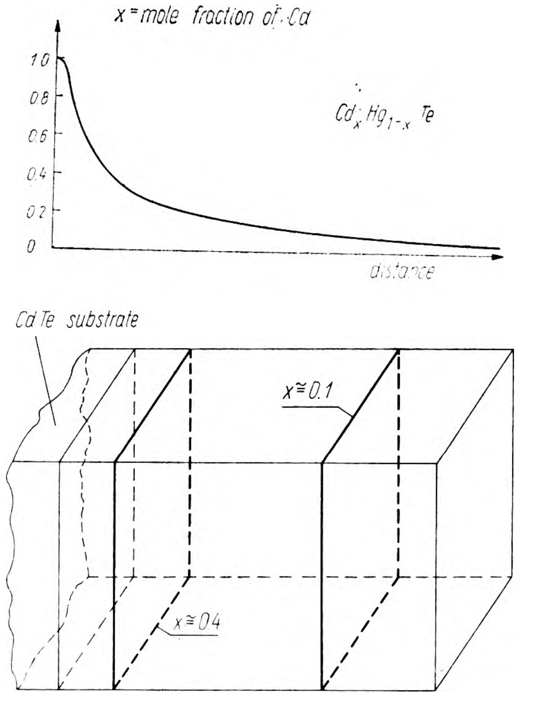

Fig. 1. A typical molar composition in the expitaxial layer [13], and an illustration of the way of cutting-out the sample with a composition gradient

defined by $0.2 < x < 0.8$. In order to improve this stoichiometry and to obtain the samples of n-type conductivity [13] a part samples prepared in this way was heated at the mercury vapour atmosphere at the temperature of 500 K. The contacts for the samples of p- and n-types have been made according to the indications given in papers [14, 15] by applying indium and gold to the n-type and p-types samples, respectively.

The measurements of the conductivity σ and the Hall voltage U_H were made by the d.c. method. During the measurements the magnetic field of induction from 0 to 0.6 Tesla were applied, while the temperature ranged from 77 to 300 K. Figs 2 and 3 show the respective results of the measurements (made on the surface with great x) for typical samples of p-type conductivity (PEM 309), and n-type conductivity (PEM 310).

For the samples of p-type (fig. 2) the Hall voltage depends strongly on magnetic field. In the magnetic field of induction $B = 0.13$ Tesla the voltage U_H changes its sign from positive to negative. In the magnetic field of induction $B > 0.13$ Tesla the voltage U_H diminishes almost linearly with the magnetic field. In strong magnetic fields, for instance, in the field of induction $B = 0.5$ Tesla the Hall coefficient changes its sign in function of temperature. However, if the magnetic induction is ten times lower the Hall coefficient is negative and remains negative within the temperature range 77—300 K. These results suggest a "mixed conductivity", i.e. contribution of both the electrons (in weak fields) and holes (dominanting in strong fields due to "exclusion" of electrons by the magnetic field) to the transport mechanism in the samples. From the measurements of Hall coefficient and conductivity we calculated the Hall mobility $\mu_H = R_H$ as a function of temperature and obtained μ_H (77 K) = 0.016 m^2/Vs for $B = 0.5$ Tesla. The value of μ_H obtained in this way concerns in principle the holes only and is in good agreement with the hole mobility value in $Cd_xHg_{1-x}Te$. For $B = 0.05$ Tesla the value of mobility μ_H (77 K) = 0.04 m^2/Vs (connected with the electron contribution to the transport) is, however, about one order of magnitude lower than that for "pure" electron mobility which for such a molar composition ($x = 0.72$) amounts to 0.5 m^2/Vs [16]. This confirms the mixed nature of the transport in the examined samples.

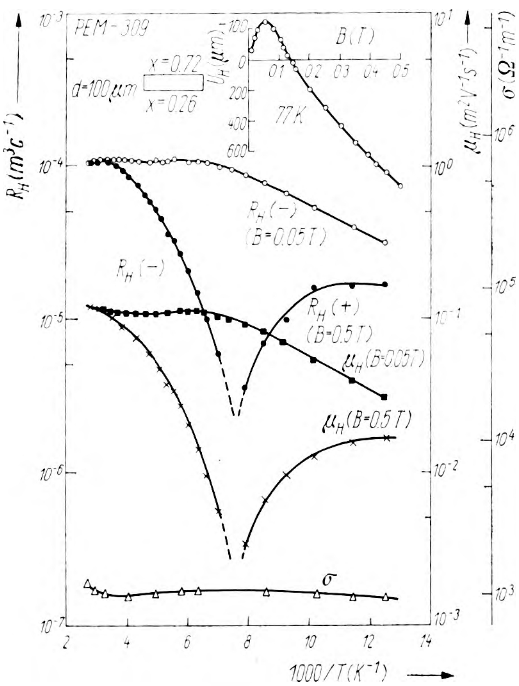

Fig. 2. Hall coefficient R_H, conductivity σ and mobility $\mu_H = \sigma R_H$ for a typical layer of p-type. The insert shows the dependence of the Hall voltage upon the magnetic field induction

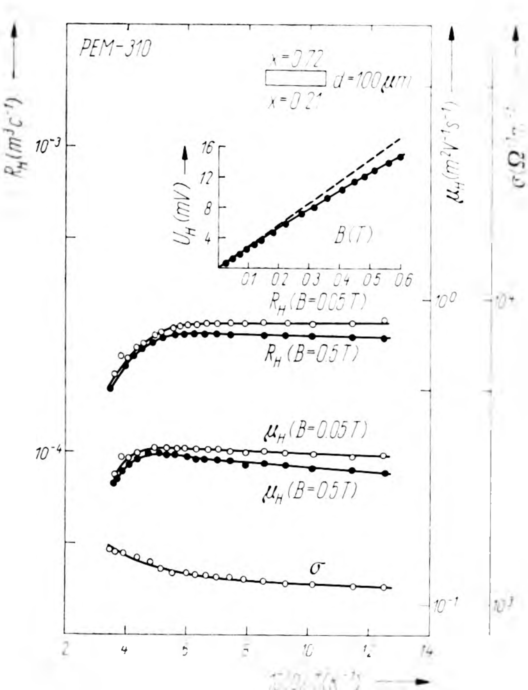

Fig. 3. Hall coefficient R_H, conductivity σ and mobility $\mu_H = \sigma R_H$ for a typical layer of n-type

For the n-type samples (fig. 3) the Hall voltage U_H does not change its sign in the magnetic field $0 < B < 0.5$ Tesla and depends almost linearly upon the field strength. The temperature dependence of the coefficient R_H does not affect the sign within the temperature range 77–300 K, and has a character typical of n-type samples. In the temperature range 77–160 K the coefficient R_H is constant but if diminishes strongly at elevated temperatures. The influence of the magnetic field on the value of R_H and on the mobility is considerably smaller than in the p-type samples. The Hall mobility in these samples was small (of order of 0.3 m^2/Vs) due to a high content of Cd. For the samples of p- and n-types the conductivity σ (of order of $10^3\ \Omega^{-1}\ m^{-1}$) was almost constant within the temperature range 77–300 K. A detailed discussion of the electric properties of the epitaxial $Cd_xHg_{1-x}Te$ layers with the parameters gradient is presented in the papers [12, 13, 17].

3.2. Spectral response of PEM-effect

The voltage measurements of the PEM-effect (U_{PEM}) have been made at two temperatures 77 K and 300 K, in a conventional measurement setup (see fig. 4) using a SMP-3 Carl Zeiss monochromator, and the magnetic field $0 < B \leqslant 2.5$ Tesla. The modulation frequency of the monochromator light flux ranged between 10 Hz and 1040 Hz*). The measure-

*) Additional measurements with the application of frequency up to 12.6 KHz have shown that the effect measured has not thermal but photon one character. In further measurement the values given above were applied.

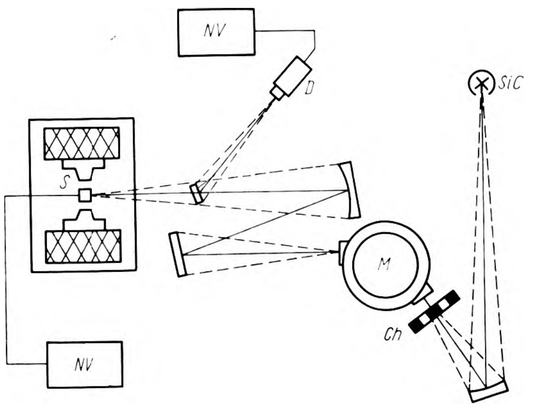

Fig. 4. Scheme of the setup used for the PEM-effect measurements. M — monochromator, SiC — radiation source of temperature 1500 K, Ch — modulator, D — reference detectors, S — sample suspensed in the magnetic field, and NV — nanovoltometer

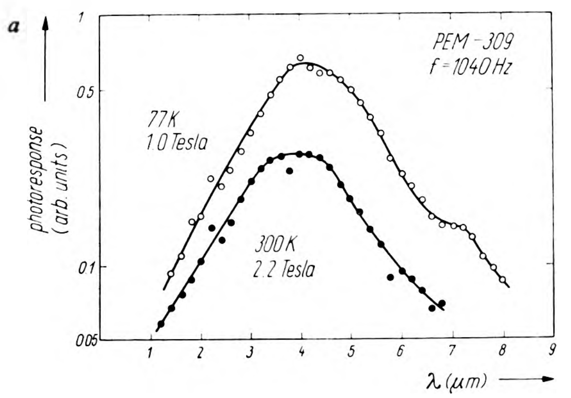

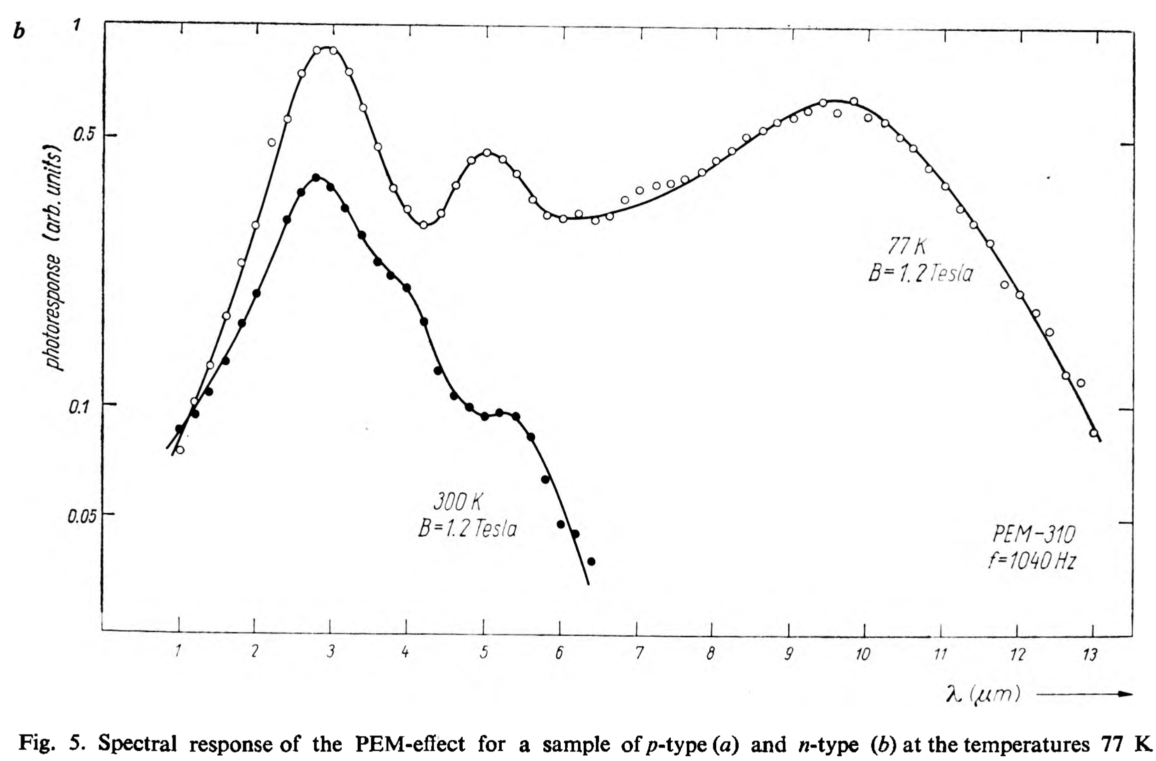

Fig. 5. Spectral response of the PEM-effect for a sample of p-type (a) and n-type (b) at the temperatures 77 K and 300 K

ments carried out allowed to determine the spectral dependence of U_{PEM} and also the dependence of photoresponses upon both the value of the magnetic field induction and the temperature.

Figs 5a and 6 show the spectral characteristics of the PEM-photoresponses for two selected layers of p- and n-types, respectively. The molar composition determined from the reflection measurement (see [13]), and given in figs 2 and 3, respectively, defines the energy gap E_g of the material on the layer boundary surfaces perpendicular to the direction of the incident radiation. At the temperature 77 K the following values of E_g have been obtained: $E_{g1} \cong 1$ eV and $E_{g2} \cong 0.18$ eV — for the p-type (PEM 305), and $E_{g1} \cong \cong 1$ eV and $E_{g2} \cong 0.09$ eV — for the n-type (PEM 310). These values restrict in practice the spectral width of the photoresponses of the examined elements as shown in the presented figures. For the prevailing majority of the layers tested the maximum photoresponses PEM have been observed in the vicinity of 3–4 μm wavelength of the radiation. The position of the maximum was practically little dependent upon the temperature. However, the long-wavelength limit of photoresponses moves distinctly towards the shorter waves as the temperature rises, which may be related to the positive temperature coefficient of the energy gap in $Cd_xHg_{1-x}Te$ for the compositions $x < 0.5$, i.e. for the material of the layer inside.

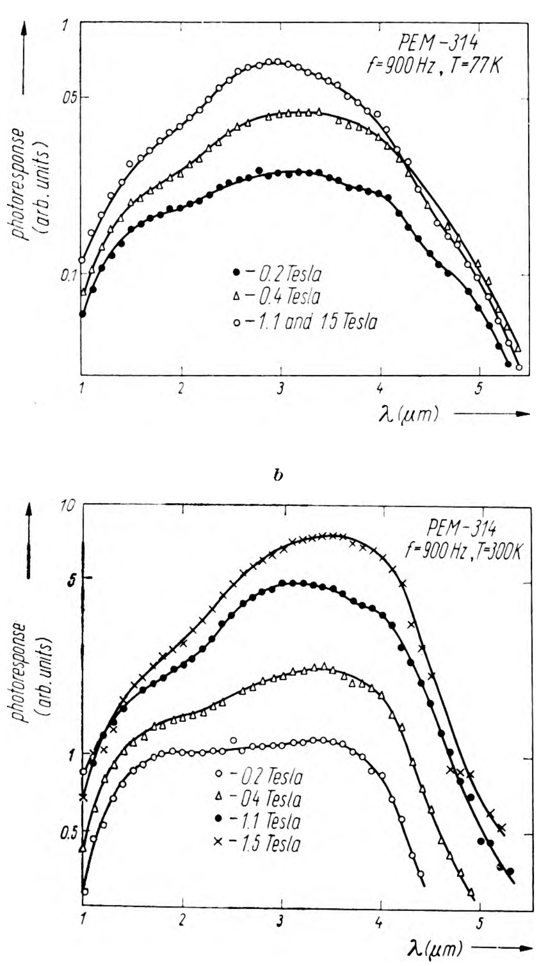

Fig. 6. The influence of the magnetic field upon the spectral characteristics of the PEM photoresponse for the sample of *p*-type at temperatures 77 K (*a*) and 300 K (*b*). The composition at the surface: $x_1 = 0.35$, $x_2 = 0.55$

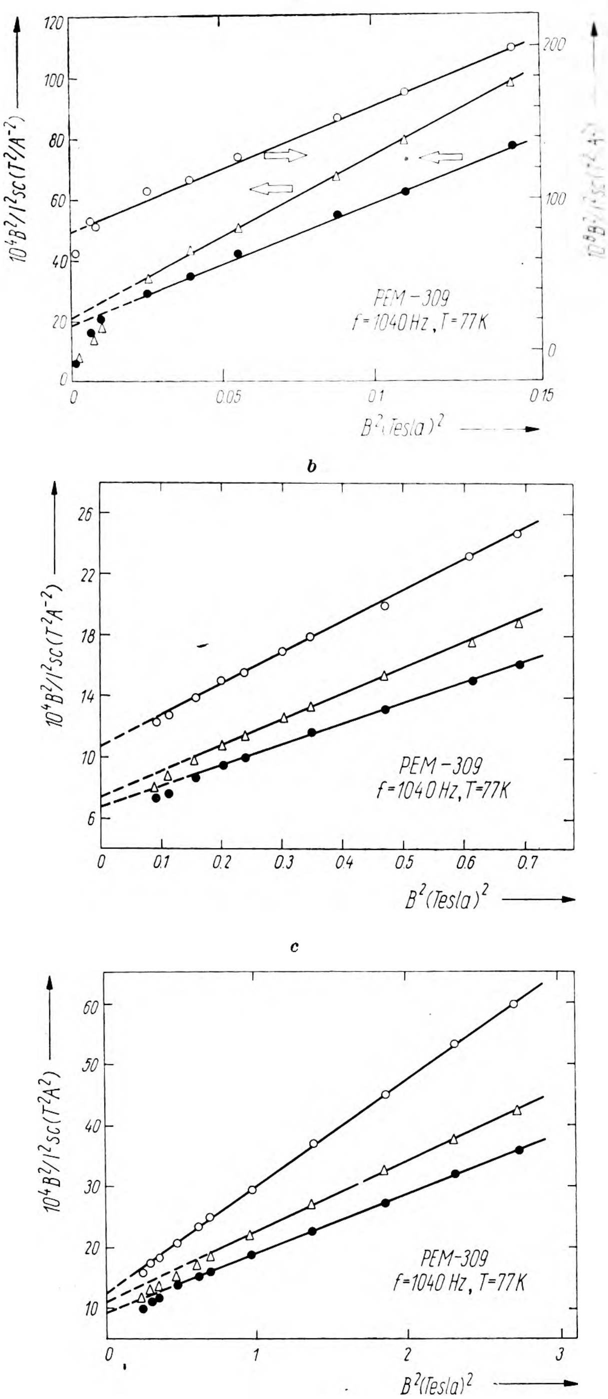

Fig. 7. The influence B^2/I_{sc}^2 upon B^2 for the layer of *n*-type for three wavelengths: triangles — 2 μm, closed circles — 3 μm and open circles — 4 μm for the weak (*a*), intermediate (*b*), and strong (*c*) ranges of magnetic fields

The influence of the magnetic field induction on the PEM-effect signal is shown in fig. 6. The deminition of the field induction *B* flattens distinctly the spectral PEM response diminishing simultaneously the absolute value of the signal. We have stated that this effect is more visible in the samples with an energy gap gradient than in monocrystals of $Cd_xHg_{1-x}Te$ in which this effect was measured for comparative reasons.

The performed measurements of the PEM photorespons dependence on the induction value *B* for selected radiation wavelengths allowed to determine the relations $B^2/I_{sc}^2 = f(B^2)$. The latters are presented in figs 7 and 8 for the layer of *p*- and *n*-types, at the presence of weak, medium and strong magnetic fields, respectively. Within each of those ranges the experimental relations may be matched to the straight line-type dependence. Next, using the formulae given in the section 2 of this work, and the slope and cut-off values of the straight lines in figs 7 and 8 the values of the PEM-effect mobilities may be determined. For the weak, intermediate and strong fields, respectively, its amount to: 3.2 – 5.3, about 1.4; 1.0–1.2, for the *p*-type; and 13.5–34.0, 3.2 – 3.9, 0.5– 1.3 — for the *n*-type (all in m^2/Vs). The mobility values obtained in this way are, of course, much greater than those measured in the transport effects (see section 3.1), because they are connected with the electrons generated by photons

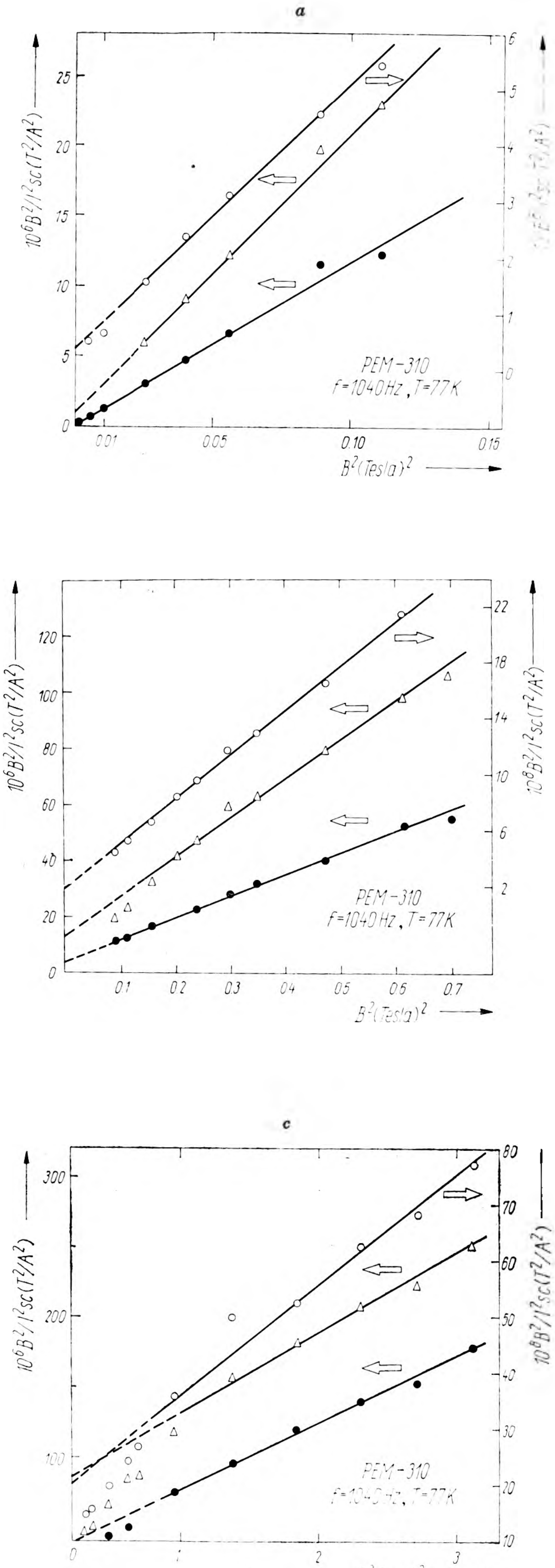

Fig. 8. The dependence of B^2/I_{sc}^2 upon B^2 in the layers of *n*-type for three wavelengths: triangles — 2 μm, closed circles — 3 μm, open circles — 4 μm, and for the weak (*a*), medium (*b*), and strong (*c*) ranges of magnetic fields

from the inside of the layer within the regions of small molar composition. As it is well known the electron mobility in the conductivity band in $Cd_xHg_{1-x}Te$ depends strongly upon the molar composition, especially for small x, achieving its maximum at 77 K at the vicinity of $x \simeq 0.16$ [16]. The presented above way of determining of the electron mobility may be particularly applicable in the examination of the properties of layer inside with the gradient of band parameters. Although the results obtained in this way are averaged over some region inside the layer but its width measured along the incident radiation direction (i.e. the width of the excitation region or, in other words, the width of interaction radiation-semiconductor) is not greater than several μm. This great (about 20 μm) is namely the averaged diffusion depth of the optically generated electrons in $Cd_xHg_{1-x}Te$ of the small molar composition range [7], on the one hand, and the width of effective absorption region of monochromatic radiation in $Cd_xHg_{1-x}Te$ with the energy gap gradient on the other one [18].

The application of the investigated layers with the gradient of energy gap to the broad-band detectors for infrared is shown in fig. 9, which shows the spectral sensitivity of the PEM-effect for the *n*-type sample.

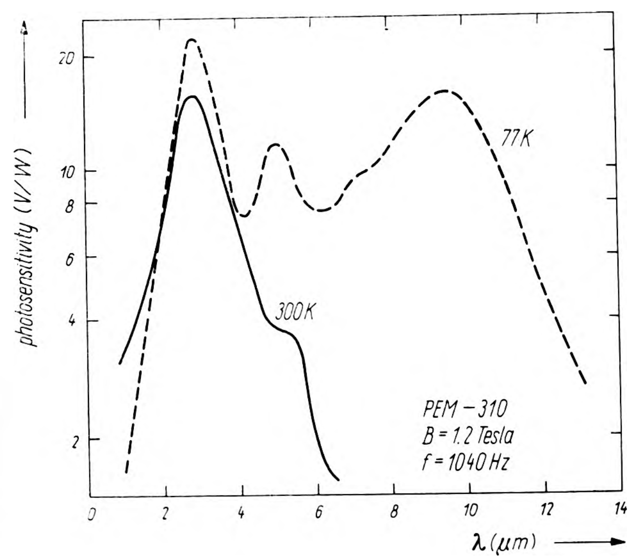

Fig. 9. Spectral sensitivity of PEM-effect for the *n*-type sample

Although the sensitivity of the PEM-effect detectors is smaller than that of photovoltaic ones with *p-n* junctions [11], the first are easier to produce. It should be also emphasized that they give relatively great value of sensitivity at the 300 K temperature in the broader wavelength band and do not require any troublesome cooling under the working conditions.

However, they require, of course, installing the magnetic field.

We have stated that the signal was essentially weaker in the samples strongly doped for the *p*-type. It may be concluded that this results from the strong volume recombination of Shockley-Reed type at low temperatures (in the vicinity of 77 K) and of Auger type at high temperatures (in the vicinity of 300 K). The highest value of the spectral sensitivity have been observed in the *n*-type samples and in those being in the intrinsic state. These samples are most suitable for infrared detectors based on PEM-effect. We have observed that the voltage noise value is small (and determines the lower level of the examined signal measurability) and the samples have relatively short reaction times. Small time constants were specially characteristic of doped layers of *p*-type.

Фотомагнитный эффект в слоях $Cd_xHg_{1-x}Te$ со ступенчатым энергетическим промежутком

Измерена спектральная характеристика фотомагнитного эффекта в эпитаксиальных слоях $Cd_xHg_{1-x}Te$ с градиентом запрещенной зоны при температурах 77-3000 K и в магнитных полях $0 < B \leqslant 2{,}5$ тл. Измерен также ток короткого замыкания фотомагнитного эффекта в функции магнитного поля. Получена информация, касающаяся свойств электрического транспорта в этих слоях и определена пригодность исследуемых элементов на широкополосные детекторы инфракрасной области.

References

[1] Kikoin I.K., Noskov M.M., Sov. Phys. **5**, 586 (1934).
[2] Van Roosbroeck W., Phys. Rev. **101**, 1713 (1956).
[3] Kurnick S.W., Zitter R.N., J. Appl. Phys. **27**, 273 (1956).
[4] Ravitsch Yu. T., *Fotomagnitnyi efekt v poluprovodnikakh i ego primenenie*, ed. Sovetskoe Radio, Moskow 1967.
[5] Kolomietz B.T., Malkova A.A., Fiz. Tverd. Tela **5**, 1219 (1963).
[6] Vdovkina E.E., Baryshev N.S., Volkova F.P., Tscherkasov A.P., Shtchetinin M.P., Averyanov I.F., Izv. AN SSSR, Neorg. Mater. **9**, 130 (1973).
[7] Marfaing Y., Chevallier J., IEEE Trans. Electron. Devices, **ED-18**, 465 (1971).
[8] Chattopadhyaya S.K. Muthur V.K., Phys. Rev. B, **3**, 3390 (1971).
[9] Chattopadhyaya S.K., Muthur V.K., Phys. Rev. B, **9**, 3517 (1974).
[10] Cohen-Solal G., Marfaing Y., Solid State Electron. **11**, 1131 (1968).
[11] Pawlikowski J. M., Becla P., Infrared Phys. **15**, 331 (1975). Becla P., Pawlikowski J.M., Infrared Phys. **16**, 457 (1976). Pawlikowski J.M., Infrared Phys. **17**, 1 (1977).
[12] Pawlikowski J.M., Becla P., phys. stat. sol. (a) **32**, 639 (1975).
[13] Pawlikowski J.M., Thin Solid Films **44** (1977).
[14] Pawlikowski J.M., Acta Physica Polon. **A49**, 139 (1976).
[15] Pawlikowski J.M., Becla P., Lubowski K., Roszkiewicz K., Acta Phys. Polon. **A49**, 563 (1976).
[16] Scott W., J. Appl. Phys. **43**, 1057 (1972).
[17] Szatkowski J., Sierański K., Pawlikowski J.M., Płaczek-Popko E., Becla P., Dudziak E., phys. stat. sol. (a) **42**, 721 (1977).
[18] Pawlikowski J.M., Becla P., Dudziak E., Opt. Appl. **VI**, 3 (1976).
[19] Pawlikowski J. M., Thin Solid Films **50** (1978).

Received, April 28, 1977